HEAT TRANSFER ON HYPERSONIC BLUNT BODIES WITH GAS INJECTION

Vladimir V. Riabov
Rivier College, Nashua, New Hampshire 03060, USA

Keywords: *heat protection; slot and uniform gas injection; hydrogen combustion; hypersonic flows*

Abstract

Numerical analysis of the gas flow in the thin viscous shock layers (TVSL) is presented under conditions of intensive gas blowing from the blunt body surface for various injection factors under the continuum and rarefied conditions. Nonequilibrium parameters in the multicomponent TVSL were evaluated for slot and uniform injections of air, helium, and hydrogen. Numerical results indicate that the most effective cooling of the probe surface occurs at moderate uniform injections and moderate Reynolds numbers.

1 Introduction

Numerical and experimental studies [1, 2] of aerothermodynamics of hypersonic vehicles showed that the temperature in the spacecraft nose region can be extremely high, and the maximum value of the heat flux occurs at small values of the nose radius R and moderate local Knudsen numbers $Kn_{\infty,R}$ and Reynolds numbers Re_0 that characterize transitional flow regimes from free-molecule medium to continuum [3]. Mass injection can be considered as an effective way of the reduction of heat transfer to the surface in this area [4].

The boundary-layer flow with gas blowing was studied in [5-7]. Only few studies [8, 9] were conducted at transitional Knudsen numbers. Moss [9] found that mass injection significantly reduces heat transfer to the surface, and when the mass injection rate equals 0.4 of the free-stream mass flux, the viscous layer is blown completely off the surface, and heat transfer is zero.

The effect of injecting gaseous coolants on heat transfer in hypersonic perfect gas flow near blunt bodies was studied in Ref. 10 on the basis of the complete system of Navier-Stokes equations, and in Ref. 9, 11, 12 on the basis of the thin viscous shock layer model [3]. Heat transfer in the presence of hydrogen blowing and combustion was studied in Ref. 13.

These studies have shown that the effectiveness of coolant blowing increases with the decrease of the Knudsen number, and becomes significant at $Kn_{\infty,R} < 0.02$. Heat transfer experimental data [12] received by the method of two-layer thermal-indicator coating confirms this conclusion. Other applications of the gas blowing include the attitude reaction control systems [14] and a counterflow drag reduction technique [15].

In the present study, the interaction of a gas flow (air and helium), blowing diffusively from a nose of the sphere opposing a hypersonic free stream, is studied numerically by the direct simulation Monte-Carlo (DSMC) technique [16-18] under the transitional rarefied-gas-flow conditions at Knudsen numbers $Kn_{\infty,R}$ from 0.016 to 1.5 and blowing factors G_w (the ratio of outgas mass flux to upstream mass flux) from 0.023 to 1.5. Combustion models of hydrogen, which is injected with different intensity from the surface of a parabolic cylinder into airflow, are considered by using the TVSL approach [3, 13] at Reynolds numbers $1500 > Re_0 > 100$.

DSMC Method

The DSMC method [16] has been used in this study as a numerical simulation technique for low-density hypersonic gas flows. The

DSMC/DS2G code (version 3.2) [17] is used for numerical calculations. Molecular collisions in air and helium are modeled using the variable hard sphere (VHS) molecular model [16]. The gas-surface interactions are assumed to be fully diffusive with full moment and energy accommodation. The code validation was tested by the author [18, 21] in comparing numerical results with experimental data [18, 21, 22] related to the simple-shape bodies. As an example, the comparison of the DSMC recent numerical results with experimental data [22] in air (without blowing) is shown in Fig. 1 for a wide range of Knudsen numbers from 0.016 to 1.5 and flow parameters: Mach number M_∞ = 6.5 and temperature factor t_w = 0.31. The error of experimental data [22] (error bars in Fig. 1) was estimated as 8-12% at different flow regimes (see Refs. 12 and 22 for details). The numerical results correlate well with experimental data at $0.016 < Kn_{\infty,R} < 0.15$.

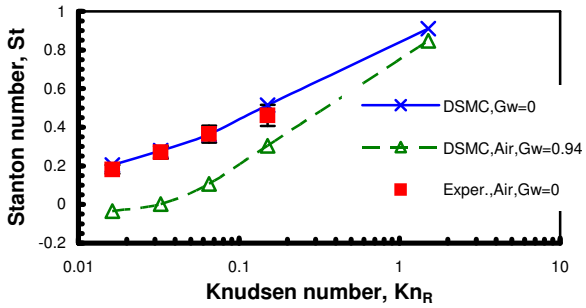

Fig. 1 Stanton number vs Knudsen number at M_∞ = 6.5 and t_w = 0.31. Experimental data are from Ref. 22.

The methodology from Refs. 16 and 17 has been applied in computations. The cases that had been considered by Bird [17] for airflow in transitional regimes were reproduced in this study. The mesh size and number of molecules per cell were varied until independence of the flow profiles and aerothermodynamic characteristics from these parameters was achieved for each considered case. In calculations at mentioned-above conditions, the total number of cells near a sphere (a half-space of the flow segment) is 4200, the molecules are distributed non-evenly, and a total number of 129,500 molecules corresponds to an average 31 molecules per cell. Following the recommendations of Refs. 16 and 17, acceptable results are obtained for an average of at least ten molecules per cell in the most critical region of the flow. The error was pronounced when this number falls below five. The cell geometry has been chosen to minimize the changes in the microscopic properties (pressure, density, and temperature) across the individual cell [16]. The variation in cell width has been based on the geometric progression principle [16] and defined by the ratio c = 20 of the width of the cell adjacent to outer boundary to the width of the cell adjacent to inner boundary. The location of the external boundary with the upstream flow conditions varies from 0.75R to 1.5R.

The DS2G program employed time averaging for steady flows [17]. About 95,000 samples have been studied in the considered cases. In all cases the usual criterion [17] for the time step Δt_m has been realized, $2\times10^{-8} \le \Delta t_m \le 1\times10^{-6}$ s. Under these conditions, aerothermodynamic coefficients and gasdynamic parameters have become insensitive to the time step. The ratios of the mean separation between collision partners to the local mean free path and the collision time ratio [17] of the time step to the local mean collision time have been well under unity over the flowfield.

Calculations were carried out on a personal computer with a Pentium® III 850-MHz processor. The computing time of each variant was estimated to be approximately 12 - 80 h.

2 Influence of the Air-blowing Factor G_w

The flow pattern over sphere is sensitive to the blowing parameter G_w. The influence of this parameter on the flow structure is studied for hypersonic airflow at M_∞ = 6.5 and $Kn_{\infty,R}$ = 0.0163. The flow conditions are the same as suggested by Botin [12] for experiments with air blowing in a vacuum chamber at stagnation temperature T_0 = 1000 K. The sphere radius is R = 0.015 m. Air is blowing diffusively from the orifice with the diameter d = 0.002 m that is located in the front critical point of the sphere. The blowing factor varies from 0 to 1.5.

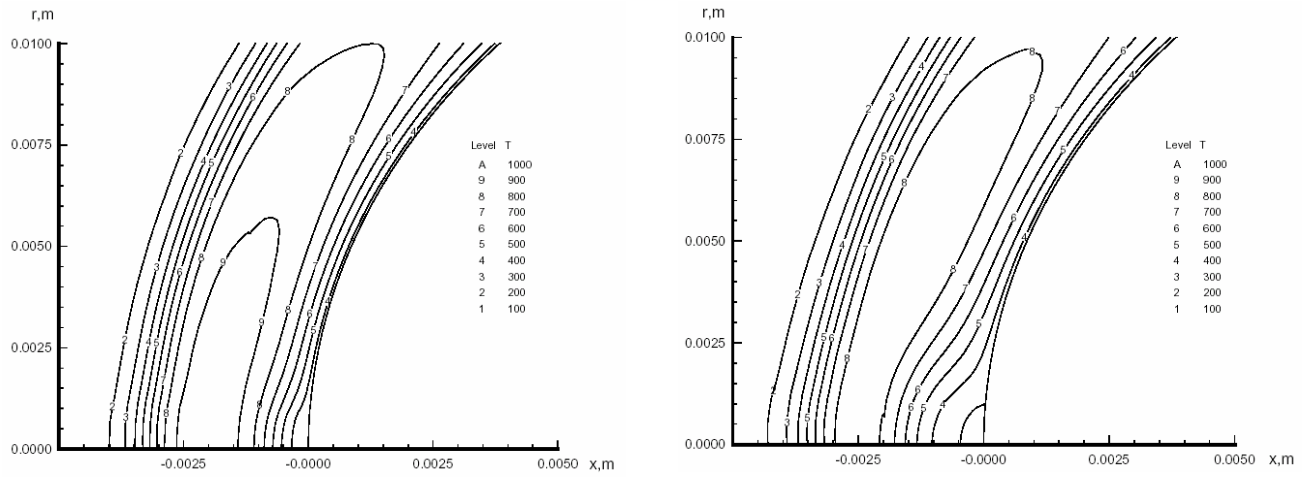

a) Air-to-air injection **b) Helium-to-air injection**

Fig. 2 Temperature contours at $Kn_{\infty,R}$ = 0.0163 and mass blowing factor G_w = 0.7.

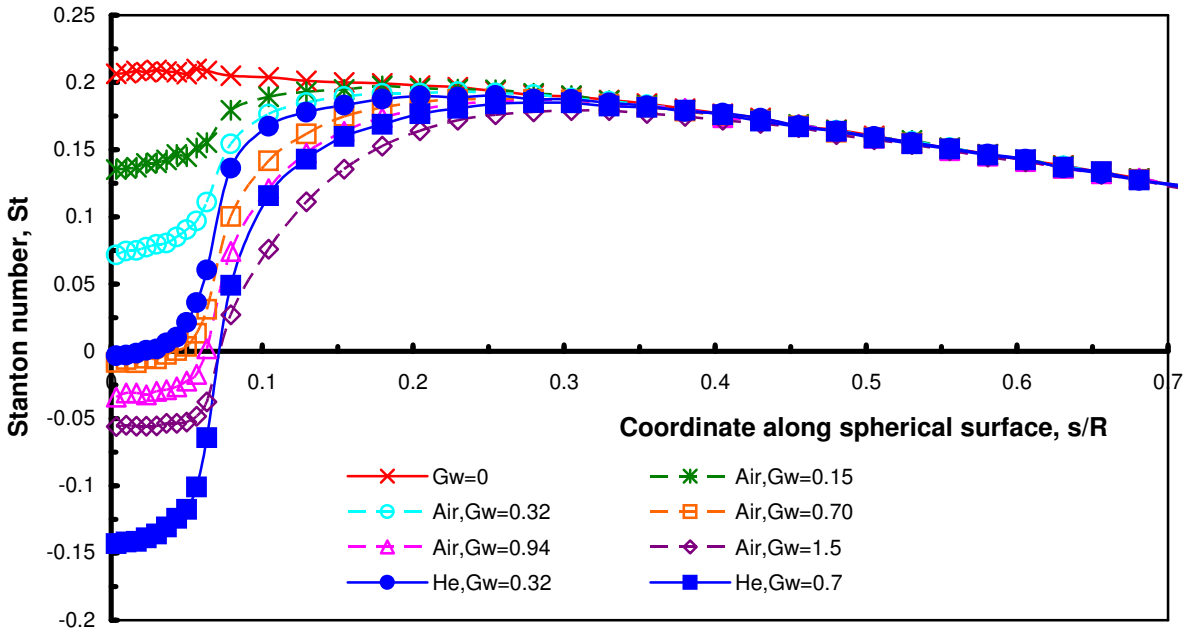

Fig. 3 Stanton number along the spherical surface at $Kn_{\infty,R}$ = 0.0163 and various air-to-air and helium-to-air mass blowing factors.

The temperature contours are shown in Fig. 2a for the case of the strong blowing factor (G_w = 0.7). The temperature field is disturbed in the vicinity of the orifice in the subsonic area of the flow behind the strong shock wave. The distributions of the Stanton number *St* along the spherical surface at various blowing factors are shown in Fig. 3. For the considered transitional flow regime conditions, when the mass injection rate equals 0.7 of the free-stream mass flux, the viscous layer is blown completely off the surface, and the heat transfer is zero.

The displacement effect spreads both in the upstream direction and along the surface. The width of the "displacement" zone can be characterized by the normalized surface coordinate $(s/R)_{max}$ where the local heat transfer is maximum, St_{max} (see Fig. 3).

3 Influence of the Rarefaction Factor

The rarefaction factor, which can be characterized by the Knudsen number, $Kn_{\infty,R}$, plays an important role in the flow structure [16-18, 21] as well as in aerothermodynamics [1-3]. The Stanton number reduces significantly with decreasing the Knudsen number (see Fig. 1). The numerical data (calculated at $G_w = 0$) correlate well with experimental data [22] at $0.015 < Kn_{\infty,R} < 0.15$. The outgas counterflow reduces significantly the heat transfer to the surface. This effect is more pronounced at lower values of the Knudsen number, $Kn_{\infty,R} < 0.075$ (see Fig. 1). Also the width of the injection-influenced "displacement" zone $(s/R)_{max}$ (at $G_w = 0.94$) increases by the factor of 3 at decreasing the Knudsen number from 1.5 to 0.015 (see Fig. 4).

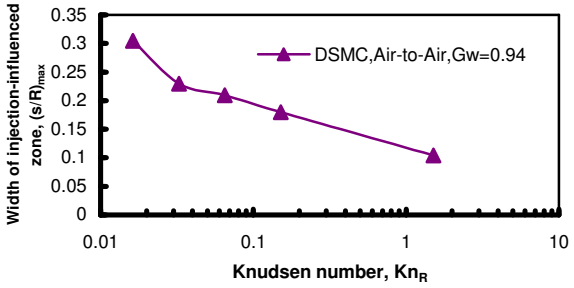

Fig. 4 Width of the injection-influenced zone, $(s/R)_{max}$ vs Knudsen number at $G_w = 0.94$.

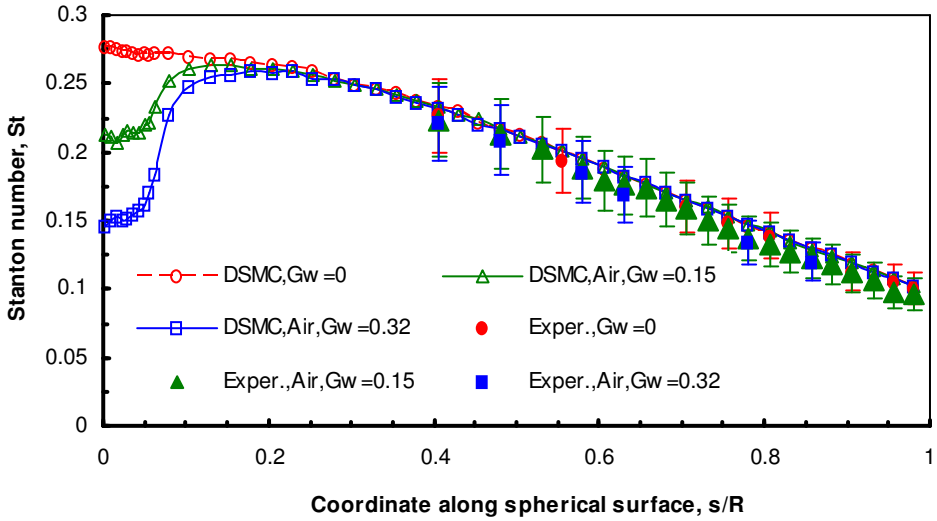

a) Air-to-air injection

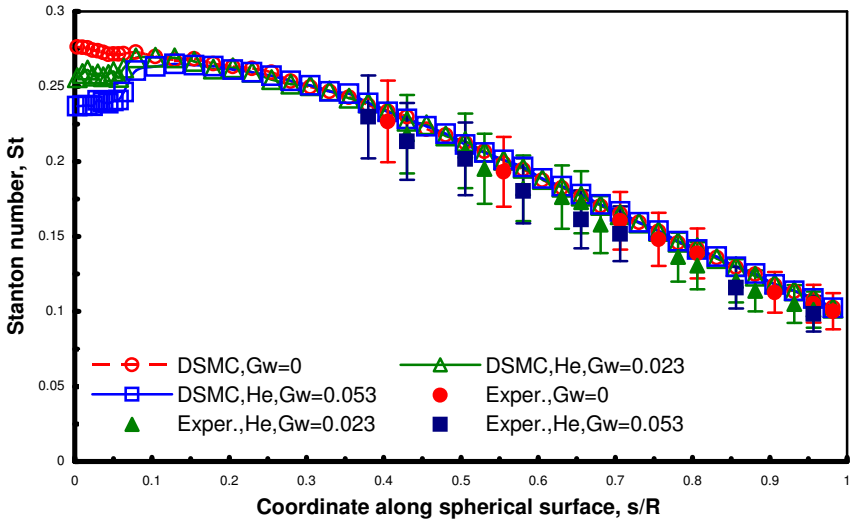

b) Helium-to-air injection

Fig. 5 Stanton number along the spherical surface at $Kn_{\infty,R} = 0.0326$ and lower mass blowing factors. Experimental data are from Ref. 12.

At lower blowing factors, numerical results correlate well with experimental data [12] that were received by the method of two-layer thermal-indicator coating [22] in a vacuum chamber at $Kn_{\infty,R}$ = 0.0326 and T_0 = 1000 K for both the air-to-air ($G_w \le 0.32$) and helium-to-air ($G_w \le 0.053$) mass injections (see Figs. 5a and 5b respectively). Under these conditions, the injection influences heat-flux distributions primarily near the orifice.

4 Diffuse Injection of Helium into Air Stream

Helium has been selected as outgas to study the role of diffusive effects of blowing. Under transitional flow conditions ($Kn_{\infty,R}$ = 0.0163), the flow structure with helium blowing has the same features as were discussed above, but the size of the "displacement" zone, $(s/R)_{max}$ is larger than in the case of air-to-air blowing due to significant differences in diffusive properties of helium and air.

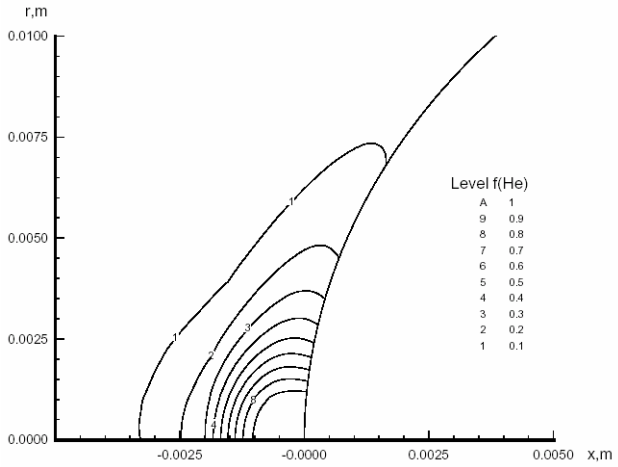

Fig. 6 Contours of helium mole fraction at $Kn_{\infty,R}$ = 0.0163 and helium-to-air blowing factor G_w = 0.7.

The temperature contours and contours of helium mole fraction f(He) are shown in Figs. 2b and 6, respectively, for the case of the strong helium mass blowing factor (G_w = 0.7). The mole concentration of helium (Fig. 6) is still significant (up to the value of 0.1) at the distance of 0.2R in the upstream-flow direction and 3.5d along the sphere surface. The temperature contours (Fig. 2b) are disturbed more pronouncedly than in the case of air-to-air blowing (see Figs. 2a). Even at moderate mass-blowing factors ($0.7 > G_w > 0.32$), diffuse outgas flow displaces completely the viscous layer off the sphere surface, and values of the Stanton number become negative (see Fig. 3). The similar effect was discussed in the experimental study by Botin [12].

5 Gas Blowing into a Boundary Layer: Continuum Flow Regime

Consider the perfect-gas flow in the boundary layer (BL) near the stagnation point of a blunt body with uniform blowing at the surface [23]. The system of BL equations acquires the following form [4, 24]:

$$U'' + fU' + \beta(S + 1 - U^2) = 0 \qquad (1)$$

$$f' = U' \qquad (2)$$

$$S'' + \sigma f S' = 0 \qquad (3)$$

where the Faulkner-Scan constant [23] $\beta = (1 + j)^{-1}$ characterizes the pressure gradient in inviscid flow; j = 0 or 1 in plane and axisymmetric cases correspondingly; and σ = 0.72 is the Prandtl number.

Boundary conditions are the following:

a) On the body surface (Y = 0) considering the gas blowing:

$$f = f_w = \text{const}, \quad U' = 0, S = S_w \qquad (4)$$

b) On the external boundary of the layer ($Y \to \infty$):

$$U = 1, \quad S = 0 \qquad (5)$$

In Eq. (4) the parameter f_w characterizes the mass flow rate of the blowing gas. Special box-schemes with uniform convergence [25] or exponential schemes [4, 24, 26] should be used in order to solve the problem at large $|f_w|$. The principal advantages of the two-point box-schemes are: 1) any type of boundary conditions "estimated" accurately [4]; 2) algorithmization of the grid-cell changes is simple [27]; and 3) fluxes of the flow parameters are calculated without additional procedure [25], and the approximation error of the fluxes is the same as

that of other terms of the equations. The two-point exponential box-scheme developed [4] has the second order of uniform convergence. The scheme and its regularization algorithm [4] have been used for the numerical solution of Eqs. (1)-(5) under the conditions of moderate and intensive blowing from the thermally isolated body surface (S_w = 0). The profiles of the tangential component of the velocity U, its derivative U', and temperature profiles g = S/S_w along the normal at the stagnation point on the surface of the axisymmetrical blunt body (β = 0.5) are shown in Figs. 7-8 for various blowing parameters (f_w = 0, –2.5, –10, –25) and temperature factors $t_w = S_w + 1$. The presence of the blowing flow significantly changes the flow structure. As the rate of blowing increases, the boundary layer becomes thicker, and the friction and heat transfer on the body surface decreases (see Fig. 9).

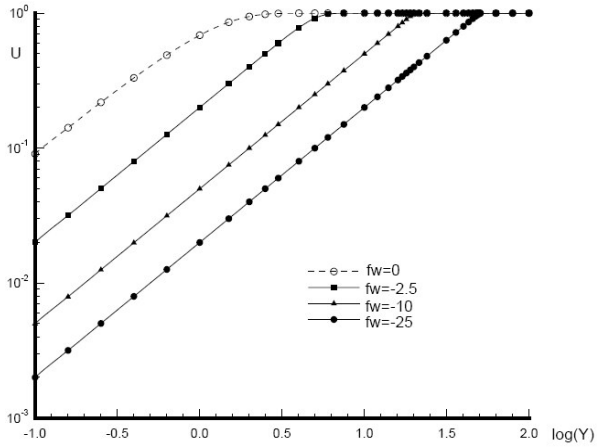

a) Function U

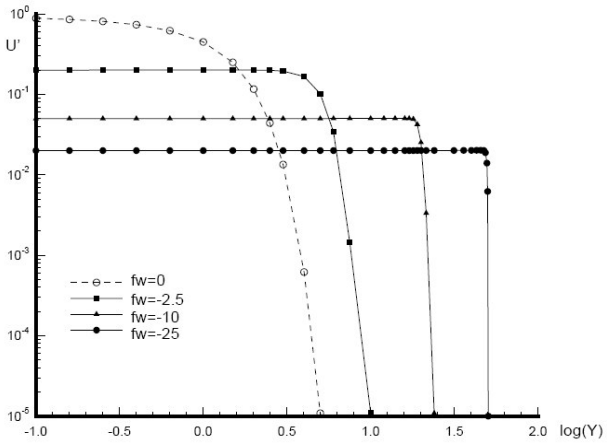

b) Function U'

Fig. 7 Functions U and U' across the boundary layer for various blowing factors at t_w = 1.

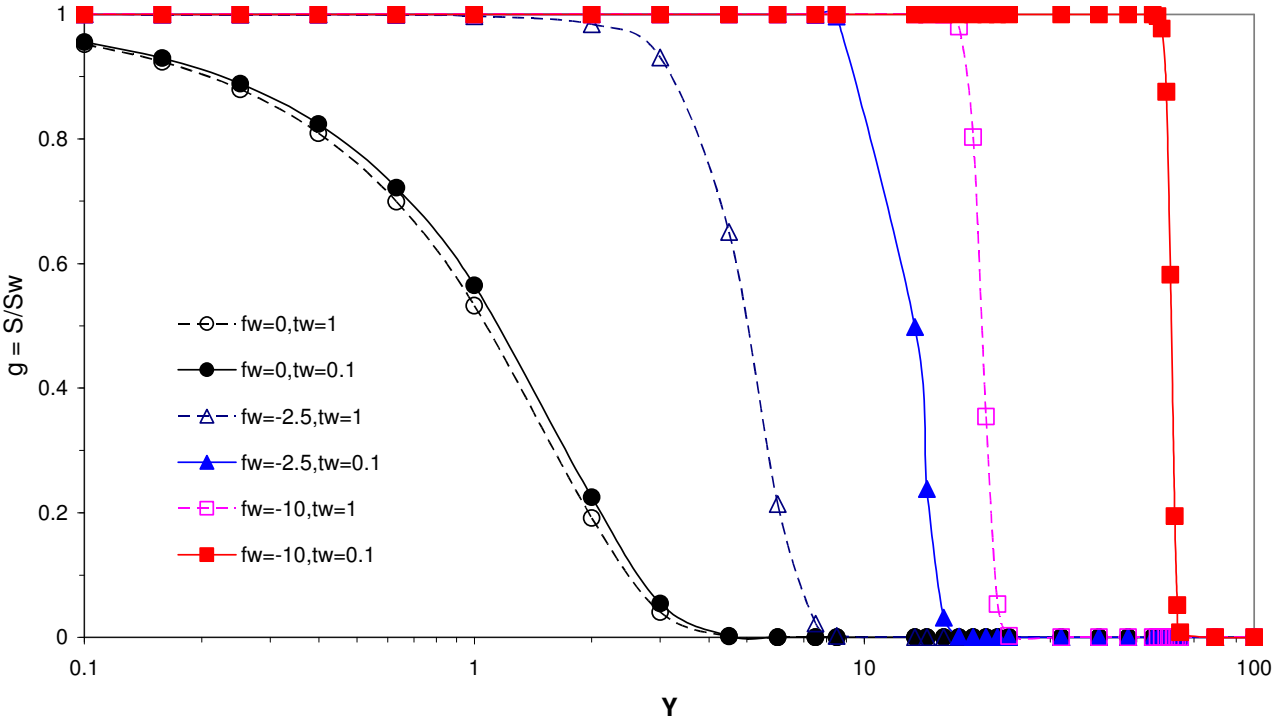

Fig. 8 Function $g = S/S_w$ across the boundary layer for various blowing (f_w) and temperature (t_w) factors.

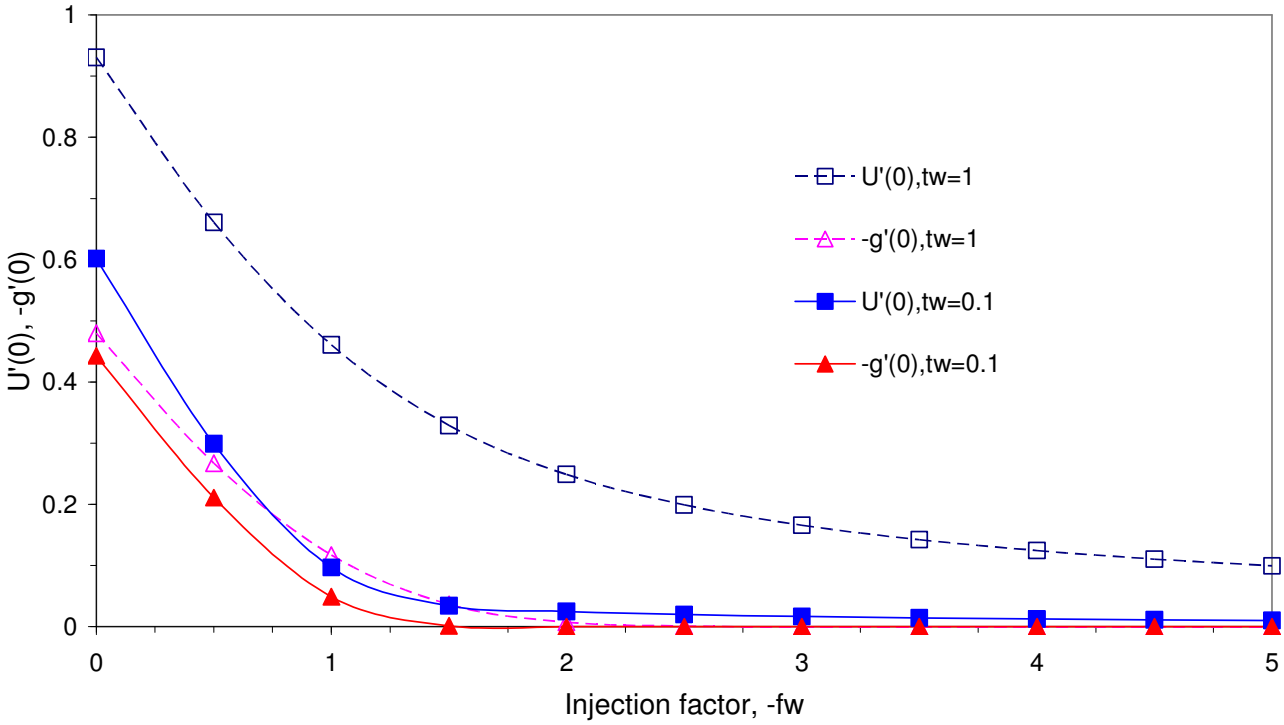

Fig. 9 Functions of friction $U'(0)$ and heat flux $g'(0)$ for various blowing (f_w) and temperature (t_w) factors.

The flow parameters in the boundary layer near cooling surface (at the temperature factor $t_w = 0.1$) with blowing are shown in Fig. 8 (solid lines). As discussed in Ref. 3, the presence of the blowing flow significantly changes the structure of the flow in the boundary layer, e.g. in the distribution of the velocity U. In addition, the essential changes in the distribution of the values $g = S/S_w$, which characterize the temperature changes, were obtained (see Fig. 8). For the $f_w = -10$ case, the main changes of the parameter g take place in the narrow zone ($1.25 < \log_{10}(Y) < 1.8$). The changes of the velocity take place in the significantly wider region ($0 < \log_{10}(Y) < 1.8$) [3]. As the temperature factor $t_w = 1 + S_w$ increases up to $t_w \approx 1$ (dashed lines in Fig. 8), the flow zone, formed by blowing, is located closer to the body surface. The transition boundary towards the upstream flow becomes wider. Without blowing, the influence of t_w on the distribution U and g is practically absent. The change of the blowing rate significantly influences the distribution of the velocity and temperature in the boundary layer, and as the result, this change significantly influences the heat flux and friction on the body surface. The complex structure of combustion zones in a thin viscous shock layer was discussed by Riabov and Botin [13] under the conditions of moderate Reynolds numbers and moderate hydrogen injections.

Figure 9 shows the parameters $g'(0)$ and $U'(0)$, which characterize the heat flux and friction on the body surface as functions of the blowing parameter f_w. The body surface is turned to be fully thermally isolated at $|f_w| \geq 2$. The further increase of the parameter $|f_w|$ is not justified. The effectiveness of the thermal isolation by blowing increases at the decreasing of temperature factor t_w from 1.0 (dashed lines) to 0.1 (solid lines). At the same time the friction decreases.

6 Combustion in the Thin Viscous Shock Layer

The analysis of hypersonic hydrogen combustion processes in the viscous shock layer near a parabolic cylinder at slot and uniform injections is based on the TVSL equations and boundary conditions [13]. Mathematical description of the nonequilibrium process of hydrogen combustion considered 11

gas components (O_2, N_2, NO, H_2O_2, HO_2, H_2O, OH, H_2, H, O, N) and 35 chemical reactions [20]. An approximation to the equations was constructed using a matrix variant of two-point exponential box-scheme [4]. Modified Newton-Raphson method [13] was used for solving the nonlinear grid equations.

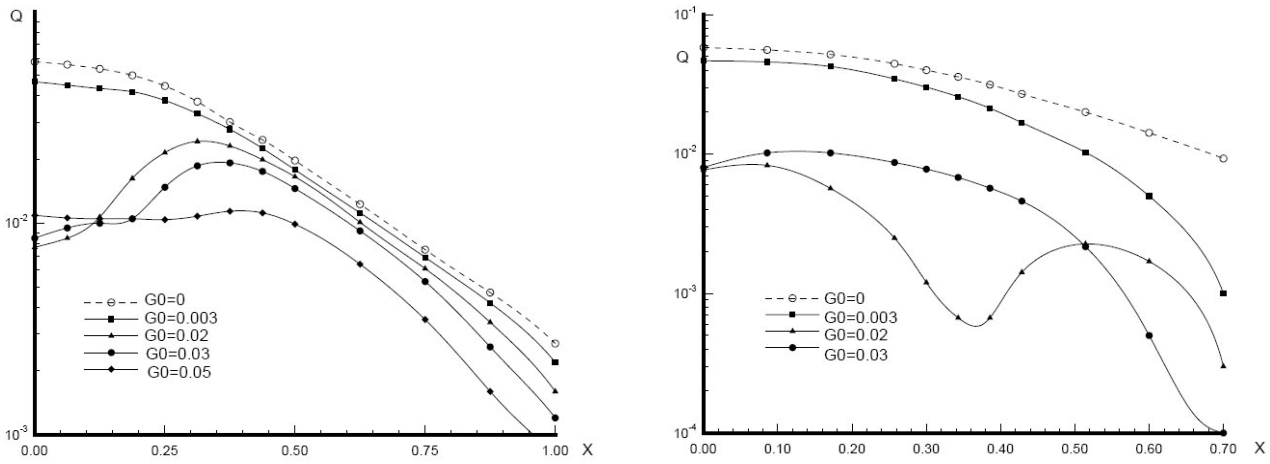

a) Slot injections **b) Uniform injections**

Fig. 10 Heat flux on parabolic cylinder at slot and uniform injections.

6.1. Slot Injection

The slot injection from the body surface was simulated by using the injection parameter $G = G_0\exp(-\alpha_w/X)$, where G_0 is the value of the parameter at the critical cylinder line, $\alpha_w = 30$, and X is marching coordinate along the surface. The computational results indicate the presence of significant amounts of nonreacting molecular hydrogen near the body. For Re_0 >100, the diffusion of the "hot" reaction products (water and *OH*) occurs from the reaction zone to the surface. This phenomenon leads to the increase of heat flux values at the surface, $Q = 2q/(\rho_\infty V_\infty^2)$ towards the body surface along the coordinate X (see Fig. 10a). The heat from combustion reactions does not prevail over the cooling effect of injection at the considered Reynolds number, $Re_0 = 628$. The heat flux is significantly lower than Q at $G_0 = 0$ near the injection zone at moderate injections ($0.02 \leq G_0 \leq 0.05$). A large quantity of injected hydrogen leads to effective cooling of the surface at a large distance from the injection zone at a high level of injection (see diamonds in Fig. 10a). The combustion zone moves from the surface towards the external boundary of the TVSL as the injection intensity increases.

6.2 Uniform Injection

Cooling the porous surface of the parabolic cylinder was modeled at $Re_0 = 628$ and the constant intensity of hydrogen injection, $G = G_0 = const$ along the surface. More significant decrease of the heat flux is found at the whole body surface, compared to the case of slot injection (see Fig. 10). For the weak injections (squares in Fig. 10b), the heat flux at the entire computational region is less than Q in the absence of the injection ($G_0 = 0$). The distribution of the heat flux becomes noticeably distinct at moderate (triangles, $G_0 = 0.02$) and strong (circles, $G_0 = 0.03$) injections, as the result of mutual influence of thermophysical properties of hydrogen, high enthalpy of upstream flow, and the presence of combustion zone in the shock layer.

Conclusions

The influence of the blowing parameter (the ratio of outgas mass flux to upstream mass flux) and the rarefaction factor (Knudsen number) on the flow structure about a sphere has been studied for hypersonic flow of air. It has been found that at transitional flow conditions ($Kn_{\infty,R}$

= 0.0163), when the mass air injection rate equals 0.7 of the free-stream mass flux, the viscous layer is blown completely off the surface, and the heat transfer is zero. The displacement effect of blowing spreads both in the counterflow direction and along the surface. This effect is more pronounced at lower values of the Knudsen number, $Kn_{\infty,R} < 0.075$. The width of the injection-influenced "displacement" zone $(s/R)_{\max}$ (at $G_w = 0.94$) increases by the factor of 3 at decreasing the Knudsen number from 1.5 to 0.016.

The temperature contours are disturbed more significantly for helium injection than in the case of air-to-air blowing. Even at moderate helium mass blowing rates ($0.7 > G_w > 0.32$), diffuse outgas flow displaces completely the viscous layer off the sphere surface.

The present results demonstrate that the moderate blowing leads to decreasing both the friction and heat flux on the surface. The flow parameters in this case should be calculated using the two-point exponential box scheme that has a property of uniform second-order convergence in the full range of blowing parameters.

The other goal was the development of a numerical tool for studying the processes of diffusive hydrogen combustion in a thin viscous shock layer at moderate Reynolds numbers. The algorithm combines a matrix factorization variant of the two-point exponential box scheme and the Newton–Raphson method for solving the nonlinear grid equations. The numerical results indicate that the major reaction products are water and *OH*, which could be used for the identification of the excess/deficient hydrogen zones. The most effective cooling of the surface occurs at moderate uniform hydrogen injection.

Acknowledgements

The author would like to express gratitude to G. A. Bird for the opportunity of using the DS2G computer program, and to V. P. Provotorov and A. V. Botin for their participation in developing numerical algorithms and fruitful discussions.

References

[1] Gnoffo P. Planetary-entry gas dynamics. *Annual Review of Fluid Mechanics*, Vol. 31, pp. 459-494, 1999.

[2] Koppenwallner G. Fundamentals of hypersonics: aerodynamics and heat transfer. *Hypersonic Aerothermodynamics*, Deutsche Forschungs- und Versuchsanstalt für Luft- und Raumfahrt E. V., Lecture Series, No. 1984-01, DFVLR-Press, 1984.

[3] Riabov V and Provotorov V. The structure of multicomponent nonequilibrium viscous shock layers. *AIAA Paper*, No. 94-2054, pp. 1-8, 1994.

[4] Riabov V and Provotorov V. Exponential box schemes for boundary-layer flows with blowing. *Journal of Thermophysics and Heat Transfer*, Vol. 10, No. 1, pp. 126-130, 1996.

[5] Warren C. An experimental investigation of the effect of ejecting a coolant gas at the nose of a blunt body. *Journal of Fluid Mechanics*, Vol. 8, Pt. III, pp. 731-744, 1960.

[6] Libby P and Gresci F. Experimental investigation of the down-stream influence of stagnation point mass transfer. *Journal of Aerospace Science*, Vol. 28, No. 1, pp. 63-72, 1961.

[7] Finley P. The flow of a jet from a body opposing a supersonic free stream. *Journal of Fluid Mechanics*, Vol. 26, No. 2, pp. 337-370, 1966.

[8] Pappas C and Lee G. Heat transfer and pressure on a hypersonic blunt cone with mass addition. *AIAA Journal*, Vol. 8, No. 8, pp. 984-995, 1970.

[9] Moss J. Reacting viscous-shock-layer solutions with multicomponent diffusion and mass injection. *NASA TR R-411*, 1974.

[10] Gershbein E and Kolesnikov A. Numerical solution of the Navier-Stokes equations in the neighborhood of the bluntness for bodies in a hypersonic rarefied gas stream in the presence of blowing. In: *Aerodynamics of Hypersonic Flows with Blowing*. Moscow State University Press, Moscow, pp. 69-77, 1979 (in Russian).

[11] Ankundinov A. Calculation of a viscous hypersonic shock layer with mass addition at moderately low Reynolds numbers. *Fluid Dynamics,* Vol.5, No. 3, pp. 40-45, 1970.

[12] Botin A. A study of local heat transfer to the spherical surface with gas injection at small Reynolds numbers. *Uchenyye Zapiski TsAGI*, Vol. 18, No. 5, pp. 41-47, 1987 (in Russian).

[13] Riabov V and Botin A. Hypersonic hydrogen combustion in the thin viscous shock layer. *Journal of Thermophysics and Heat Transfer*, Vol. 9, No. 2, pp. 233-239, 1995.

[14] Gimelshein SF, Alexeenko AA and Levin DA. Modeling of the interaction of a side jet with a rarefied atmosphere. *Journal of Spacecraft and Rockets*, Vol. 39, No. 2, pp. 168-176, 2002.

[15] Josyula E, Pinney M and Blake WB. Applications of a counterflow drag reduction technique in high-speed systems. *Journal of Spacecraft and Rockets*, Vol. 39, No. 4, pp. 605-614, 2002.

[16] Bird G. *molecular gas dynamics and the direct simulation of gas flows*, Oxford Univ. Press, 1994.

[17] Bird G. The DS2G program user's guide. G.A.B. Consulting Pty, Killara, NSW, Australia, 1999.

[18] Riabov V. Comparative similarity analysis of hypersonic rarefied gas flows near simple-shape bodies. *Journal of Spacecraft and Rockets*, Vol. 35, No. 4, pp. 424-433, 1998.

[19] Riabov V. Heat transfer on a hypersonic sphere with diffuse rarefied-gas injection. *Journal of Spacecraft and Rockets*, Vol. 41, No. 4, pp. 698-703, 2004.

[20] Dimitrov V. *Simple kinetics*. Moscow: Nauka, 1982.

[21] Riabov V. Aerodynamics of two side-by-side plates in hypersonic rarefied-gas flows. *Journal of Spacecraft and Rockets*, Vol. 39, No. 6, pp. 910-916, 2002.

[22] Ardasheva MM, Klimova TV, Pervushin GE and Chernikova LG. Application of a two-layer thermal-indicator coating for investigating heat transfer in vacuum wind tunnels. *Uchenyye Zapiski TsAGI*, Vol. 10, No. 6, pp. 79-87, 1979 (in Russian).

[23] Schlichting H. *Boundary-layer theory*, 7th edition. New York: McGraw-Hill, 1979.

[24] Liu TM and Chiu HH. Fast and stable numerical method for boundary-layer flow with massive blowing. *AIAA Journal*, Vol. 14, No. 1, pp. 114-116, 1976.

[25] Keller HB. Accurate difference methods for nonlinear two-point boundary value problems. *SIAM Journal of Numerical Analysis*, Vol. 11, No. 2, pp. 305-320, 1974.

[26] El-Mistikawy TM and Werle MJ. Numerical method for boundary layers with blowing – the exponential box scheme. *AIAA Journal*, Vol. 16, No. 7, pp. 749-751, 1978.

[27] Provotorov VP. A new regularization algorithm for numerical solution of the thin-viscous-shock-layer equations. *Trudy TsAGI*, No. 2436, pp. 165-173, 1990 (in Russian).

Copyright Statement